

Magnetic state of $\text{La}_{1.36}\text{Sr}_{1.64}\text{Mn}_2\text{O}_7$ probed by magnetic force microscopy

Junwei Huang,¹ Changbae Hyun,^{1,*} Tien-Ming Chuang,^{1,†} Jeehoon Kim,^{1,‡} J. B. Goodenough,² J.-S. Zhou,² J. F. Mitchell,³ and Alex de Lozanne^{1,2,§}

¹Department of Physics, University of Texas, Austin, Texas 78712, USA

²Texas Materials Institute, University of Texas, Austin, Texas 78712, USA

³Materials Science Division, Argonne National Laboratory, Argonne, Illinois 60439, USA

(Received 16 October 2007; revised manuscript received 6 December 2007; published 4 January 2008)

We have investigated the ferromagnetic (FM) domain structure of a single-crystal bilayered manganite $\text{La}_{2-2x}\text{Sr}_{1+2x}\text{Mn}_2\text{O}_7$ ($x=0.32$) by using low-temperature magnetic force microscopy. We observed that below 65 K, the FM domains form stable treelike patterns with out-of-plane magnetization. With increasing temperature, the FM domain patterns gradually change in the form of domain wall motion. Above 80 K, the FM domain patterns change more and more with each temperature step. The magnetization changes from the out-of-plane to an in-plane direction around 88 K. The in-plane FM domains almost completely disappear near the Curie temperature of this sample ($T_C \approx 110$ K), where the resistivity exhibits a sharp increase. We also observed large changes in the magnetic structures upon thermal cycling. We concluded that the formation of FM domains at low temperatures ($T < 80$ K) is determined by the energy associated with surface magnetic free poles and domain walls. At high temperatures ($80 \text{ K} < T < T_C$), the two-dimensional FM fluctuations in the basal plane may also play an important role in forming the domain structures. The evolution of the FM domain patterns with temperature coincides with the change in resistivity.

DOI: [10.1103/PhysRevB.77.024405](https://doi.org/10.1103/PhysRevB.77.024405)

PACS number(s): 75.47.Lx, 68.37.Rt

I. INTRODUCTION

The mixed-valent perovskite manganites, such as $\text{La}_{1-x}\text{Sr}_x\text{MnO}_3$ and $(\text{La},\text{Pr})_{1-x}\text{Ca}_x\text{MnO}_3$ in a certain hole doping region, exhibit a phase transition from a paramagnetic or antiferromagnetic insulating phase to a ferromagnetic (FM) metallic phase;¹⁻³ upon cooling through the Curie temperature, FM clusters first form in the paramagnetic matrix and grow to merge and form a percolative path through the whole sample below T_C .⁴⁻⁶ In this process, the formation of FM clusters can be strongly affected by an external magnetic field. As the FM clusters percolate through the whole sample, e.g., as in $\text{La}_{2/3}\text{Ca}_{1/3}\text{MnO}_3$, a tremendous drop in resistivity occurs accompanied by a discontinuous decrease in the equilibrium Mn-O bond length, signaling a first-order phase transition from insulating to metallic behavior.^{7,8} This percolation mechanism in perovskite manganites has been confirmed by various measurements such as neutron scattering,⁵ transport,⁶ and magnetic force microscopy (MFM).⁹ Compared to FM perovskite manganites, the bilayered manganites $\text{La}_{2-2x}\text{Sr}_{1+2x}\text{Mn}_2\text{O}_7$ ($0.30 < x < 0.50$) exhibit more complicated FM ground states as a function of the hole doping x , because of the two dimensionality of the system.¹⁰ In the FM ground state, the easy axis of magnetization is along the c axis for hole concentrations $x < 0.32$, but switches to the ab plane for hole concentrations $x > 0.32$. The $x=0.32$ composition is at the crossover from the out-of-plane magnetization to the in-plane magnetization. The magnetic structures in this composition were found to be significantly affected by the change in external parameters such as pressure, temperature, and magnetic field.^{11,12} Welp *et al.*¹² observed that a spin reorientation transition (SRT) occurs in the $x=0.32$ compound around 80 K by using magnetization measurements; the easy axis of the crystal tilts away from the c axis toward the ab plane. They attributed this change to a

decrease of the first-order and second-order anisotropy constants with increasing temperature. They also observed maze-shaped domains in the ab plane below 75 K by using magneto-optical imaging. Recently, Asaka *et al.*¹³ observed magnetic ripple and nanowidth domains evolving with temperature in the $x=0.32$ compound by using Lorentz transmission electron microscopy (LTEM). The evolution of magnetic domains indicated that the SRT occurs in the interval 55–70 K. They argued that the SRT is caused by the two-dimensional fluctuations of magnetic moments in the basal plane and the orbital occupancy transition from the $d_{3z^2-r^2}$ to the $d_{x^2-y^2}$ orbitals. By using low-temperature MFM, we have performed systematic magnetic measurements of the (001) plane of a single crystal $x=0.32$ compound from 30 to 110 K (T_C) under various external magnetic fields in order to explore the evolution of FM domains with temperature and magnetic field. Interestingly, we observed nanosized, treelike magnetic domain patterns evolving with temperature and magnetic field.

II. CRYSTAL SYNTHESIS, CHARACTERIZATION, AND MAGNETIC FORCE MICROSCOPY DETAILS

Single crystals of $\text{La}_{1.36}\text{Sr}_{1.64}\text{Mn}_2\text{O}_7$ were grown by the traveling floating zone method in an image furnace at the Argonne National Laboratory. Magnetization measurements under 250 Oe magnetic field in a dc superconducting quantum interference device (Quantum Design) show a ferromagnetic transition at $T_C \approx 110$ K. The sample was cleaved along the ab plane in air before being loaded onto the sample stage of a homebuilt, low-temperature magnetic force microscope.^{14,15} The cleaved sample shows a mirrorlike flat surface. The MFM tips were prepared by coating a layer of 35 nm thick Co/Cr magnetic material onto commercial

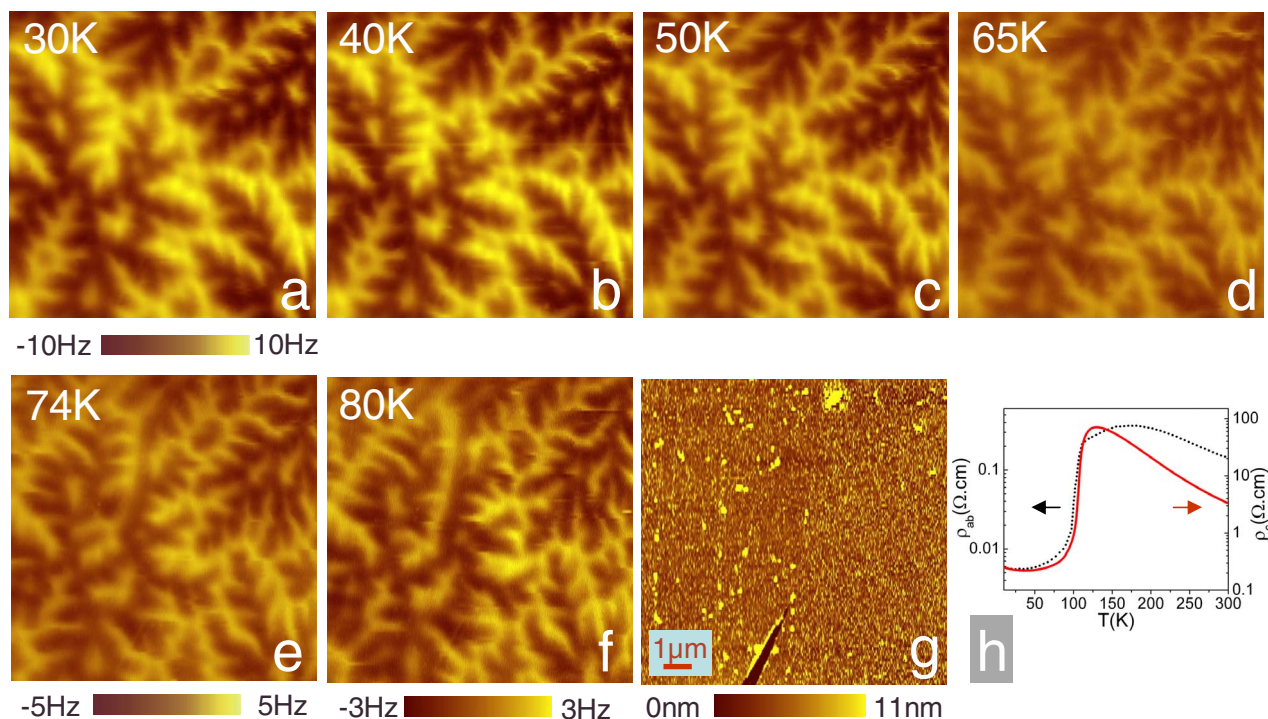


FIG. 1. (Color online) Evolution of magnetic domain structures in $\text{La}_{1.36}\text{Sr}_{1.64}\text{Mn}_2\text{O}_7$ with temperature from 30 to 80 K. (a)–(f) are MFM images taken at the area shown in (g) at various temperatures under zero field. Thermal drift of the tip with respect to the sample occurring during the measurement was compensated by the tube scanner offset. (g) is the topography with size $15 \times 15 \mu\text{m}^2$. (h) is the resistivity data in the ab plane (dotted) and the c axis (solid) reported in Ref. 11 for the same samples. In MFM images, the magnetic force gradient generated by magnetic domains is expressed in terms of the resonant frequency shift of the cantilever, and is displayed in the color scale. A repulsive magnetic force results in a positive frequency shift, while an attractive magnetic force results in a negative frequency shift.

atomic force microscopy tips with rf-magnetron sputtering. These tips were then magnetized by a strong permanent magnet so as to have the magnetic moment pointing toward the sample. The MFM chamber was first pumped down to 1×10^{-6} torr and then filled with ~ 350 mtorr of helium exchange gas. The helium exchange gas was used not only for fast cooling of the MFM body, but also for stabilizing the MFM measurements. The whole MFM probe was placed inside a cryogenic Dewar. The MFM images presented in this paper were obtained in a linear mode with about 80 nm lift height.

III. MAGNETIC FORCE MICROSCOPY RESULTS

A. Temperature dependence of the micromagnetic properties

Figures 1(a)–1(f) show the evolution of the magnetic domains with temperature from 30 to 80 K under zero magnetic field. The sample was zero-field cooled from room temperature down to 30 K. The measurement was conducted in a warming up run. At 30 K, FM domains with out-of-plane magnetization form treelike patterns with 180° domain wall structures. Bright and dark areas are domains with magnetization pointing out of and into the sample, respectively. The width of the domains ranges from 200 to 500 nm, which is consistent with the domain size observed by Asaka *et al.*¹³ Such FM domain patterns are very similar to the ones observed on the (001) surface of cobalt, a uniaxial fer-

romagnet.^{16,17} The formation of these magnetic domain patterns can be interpreted by considering the energies associated with the surface free magnetic poles and the domain walls.¹⁸ The total energy is minimized when the reduction in magnetostatic energy due to having smaller domains matches the energy spent in creating new domain walls. With increasing temperature from 30 to 65 K [Figs. 1(a)–1(d)], the domain patterns remain stable, but the magnetization of the domains gradually decreases as is to be qualitatively expected from a Brillouin function¹⁹ (note the scale bars). The domain walls start to show an apparent movement at 74 K (refer to the middle of the MFM images), which indicates that the previously energy-balanced magnetic state breaks down and a different balanced magnetic state shows up. The motion of domain walls is dominantly driven by the competition between the surface magnetic free-pole energy and domain wall energy. Since the magnetic free-pole energy depends on the component of the magnetization perpendicular to the (001) plane, changes may be partially driven by the change in the easy axis direction due to the temperature-dependent first-order and second-order anisotropy constants. This change is indicative of the onset of the SRT. At higher temperatures, the domains change increasingly more from one temperature step to the next [Fig. 1(f)]. Above 80 K, we took MFM images with smaller temperature steps in order to obtain a detailed picture of the evolution of the spin moment with temperature.

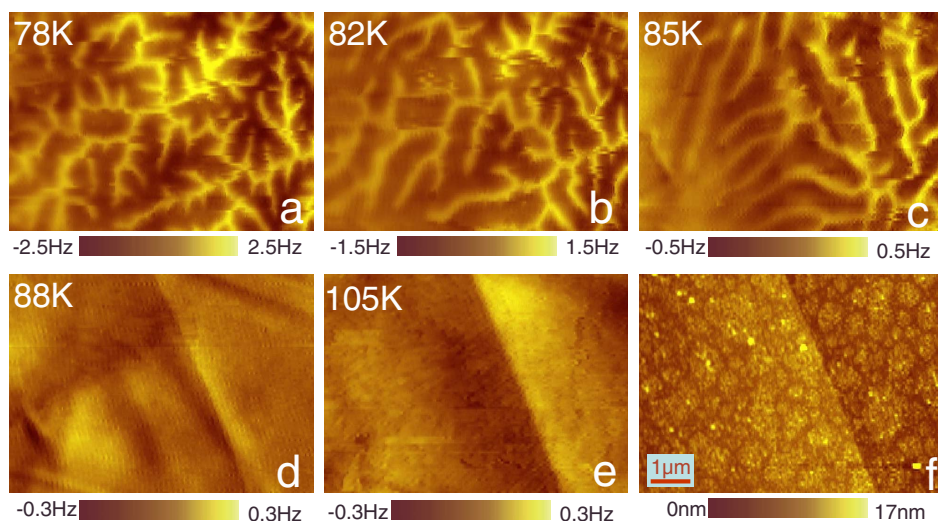


FIG. 2. (Color online) Evolution of magnetic domain structures in $\text{La}_{1.36}\text{Sr}_{1.64}\text{Mn}_2\text{O}_7$ with temperature from 78 to 105 K. The sample was zero-field cooled from room temperature down to 78 K. The MFM images were taken in a warming up run. (a)–(e) are MFM images taken at the area shown in (f) under zero field. (f) is a topographic image with size $8 \times 6 \mu\text{m}^2$. The step shown in the MFM images in (d) and (e) is due to the topographic effect, which occurs when the magnetic signal is weak.

B. Observation of the spin reorientation transition

Figure 2 shows a series of MFM images taken at a different position from that shown in Fig. 1. As the temperature increases from 78 to 85 K [Figs. 2(a)–2(c)], we can see that the small wavy domains merge into larger domains at elevated temperatures; curved domain walls change their stretching directions on the surface in such a manner that they tend to form parallel stripes. As is well known, for a domain with magnetization perpendicular to the crystal surface, the domain width is approximately proportional to $\gamma^{1/2}/M_s$ (γ is domain wall energy per unit area, M_s is magnetization).¹⁹ So it is expected that the domain width will change as the domain wall energy and the magnetization change with temperature. Below 88 K, the major component of the magnetization is still out of plane. As the temperature is raised up to 88 K [Fig. 2(d)], only in-plane domains appear on the sample surface. This signals that the SRT finishes around 88 K in this sample. While MFM alone is not able to determine all the components of the magnetization, our conclusion about the SRT is based on our MFM data and on previous observations.^{12,13} The in-plane domains become weaker and weaker at higher temperatures until they disappear around the Curie temperature [Fig. 2(e)] as expected. MFM cannot image in-plane domains, but their domain walls do produce clear contrast, as in Permalloy squares¹⁵ and computer hard disks.²⁰

In perovskite manganites exhibiting a colossal magnetoresistance, the formation of FM domains coincides with the change in resistivity. Transport measurements on the $x=0.32$ compound have shown that the resistivity [Fig. 1(h)] along the c axis and in the ab plane remain almost constant below 60 K.¹¹ The resistivity gradually increases from 60 to 100 K and exhibits a sudden increase near the Curie temperature (110 K) due to a metal-insulator transition. These are the same samples used in our study. Our MFM results in Figs. 1 and 2 show that the FM domain patterns remain very stable below 65 K, which coincides with a nearly constant resistivity. The domain walls start to move with their magnetization remaining mostly out of plane as the temperature increases from 65 to 88 K, which coincides

with the gradual increase in resistivity. Above 88 K, the magnetization of the domains tilts away from the out-of-plane direction, signaling a change in the direction of the easy axis that does not occur in mixed-valent perovskite manganites such as $\text{La}_{1-x}\text{Sr}_x\text{MnO}_3$. The change in the direction of the easy axis of the $x=0.32$ compound is due to the change in the sign of the first-order crystal anisotropy constant of this compound near 80 K.¹² The detailed evolution of domains cannot be easily obtained with our MFM measurements above 88 K because of the complexity of the in-plane domain patterns and the relative difficulty in imaging in-plane domains with MFM. In the neighborhood of the FM transition, $T \approx T_C$, the in-plane domains vanish gradually and the resistivity increases dramatically. However, the detailed electronic and magnetic structures within domains should be chiefly responsible for the change in resistivity with temperature.²¹ Our MFM results show that the SRT occurs from 74 to 88 K, which is different from what Asaka *et al.* observed in the same composition by using LTEM.¹³ The domain patterns we observed are more complicated than the nanosized ripples reported by them. The difference is likely due to sample preparation. For the LTEM study, the sample needs to be ground down to 150 nm or less. This grinding process creates many defects and strain in the sample, which inevitably influences the SRT. Furthermore, as the sample becomes thin, the shape anisotropy energy will play an important role in the magnetostatics, favoring in-plane magnetization. It is also possible that small changes in doping (x) make significant changes in the SRT temperature, since a change from $x=0.31$ to $x=0.33$ changes the magnetization from out-of-plane to in-plane direction without a SRT.²² Neutron powder diffraction experiments showed that the spin moment stays almost along the c axis at low temperatures, gradually tilts away from the c axis with increasing temperature, and forms a maximum angle of about 50° with the c axis at 90 K,²³ which was already confirmed by the macroscopic magnetization measurement.¹² Our MFM results obtained from 30 to 88 K are consistent with these measurements. However, at $90 \text{ K} < T < T_C$, the domains within a thick layer near the surface are aligned in-plane due to demagnetizing fields and the tilted easy axis. MFM picked the

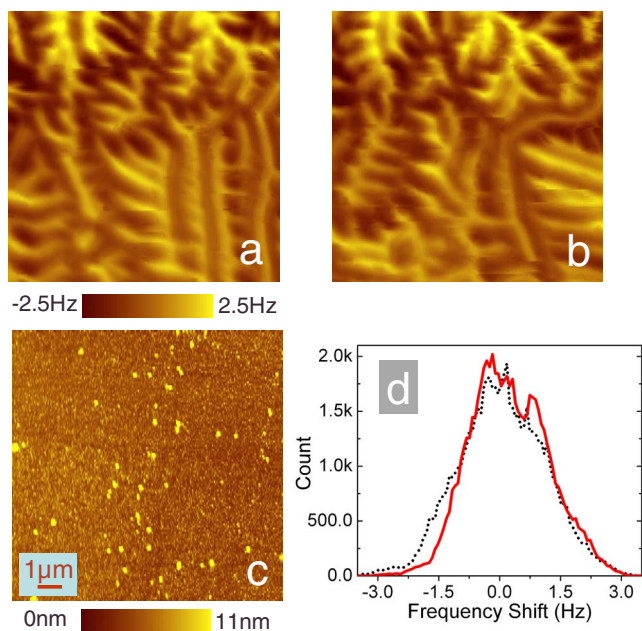


FIG. 3. (Color online) Thermal cycling behavior observed in the magnetic structures in $\text{La}_{1.36}\text{Sr}_{1.64}\text{Mn}_2\text{O}_7$ under zero field. The sample was zero-field cooled from room temperature down to 78 K. (a) and (b) are MFM images taken at the area shown in (c) at initial 78 K and final 78 K, respectively. (c) is topography with size $(8.6 \mu\text{m})^2$. (d) is a histogram of the MFM images (a) (dotted curve) and (b) (solid curve).

magnetic signals only from these in-plane surface domains, which explains why our MFM results obtained above 88 K show in-plane domains, while the neutron powder diffraction and magnetization measurements showed tilted domains.

C. Micromagnetic thermal irreversibility

Another interesting result we observed is the domain behavior upon thermal cycling in zero magnetic field. The sample was zero-field cooled from room temperature down to 78 K. The thermal cycle started at 78 K, went through 82 K, and came back to 78 K. MFM images taken at the initial 78 K and final 78 K show significant difference in domain structure [see Figs. 3(a) and 3(b)], but the total magnetic domain distribution in the area shown in Fig. 3(c) does not change, as seen from the histogram of Fig. 3(d). The domains with stronger magnetization (brighter areas at the upper left part of the images) underwent less change than the weaker domains. The nanoscale thermal cycle dependence of the magnetic structure in this compound has not been previously reported. This behavior is evidence of the existence of a partial destruction and nucleation of domain wall area on thermal cycling that depends on the preexisting domain pattern, which may also indicate temperature-dependent two-dimensional ferromagnetic fluctuations.

D. Evolution of magnetic domains with external field

In the presence of external magnetic fields, we measured the magnetic domain structures in the sample at 78 K and at 88 K. The field was applied perpendicular to the sample surface along the tip magnetic moment. Figure 4(a) was taken under zero field. When the field was applied up to 185 G, the volume of the domains parallel to the field was seen to grow [Fig. 4(b)], which results in the increase in the dark area and decrease in the bright area. We believe the main component of the magnetization is still out of plane at 78 K. At 88 K, the MFM images in Figs. 4(d) and 4(e) show that the magnetization of most domains is in-plane. The magnetic signal generated by the in-plane domains is much weaker than the signal generated by the out-of-plane domains in Figs. 4(a)

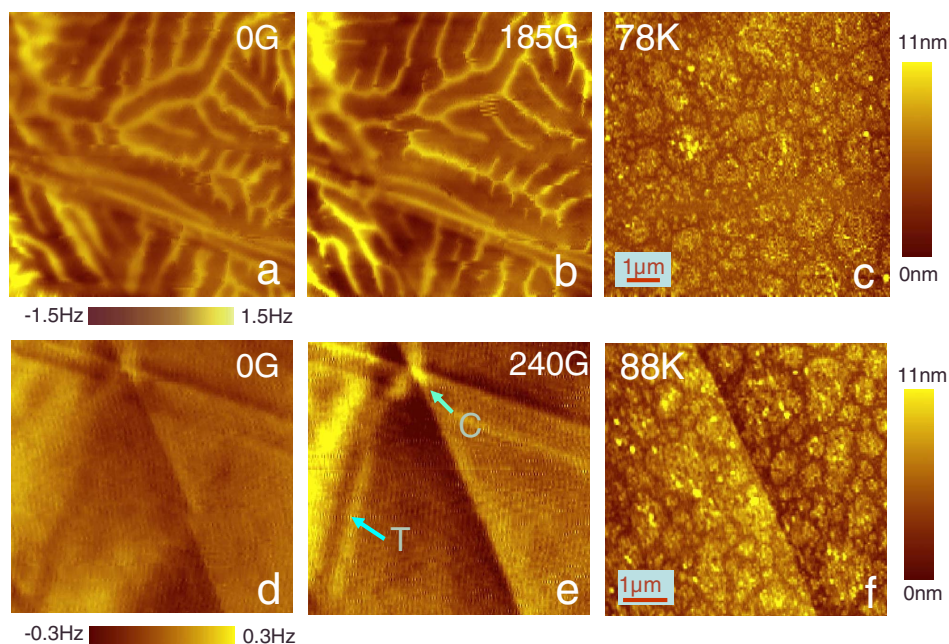


FIG. 4. (Color online) Evolution of the magnetic domain structures in $\text{La}_{1.36}\text{Sr}_{1.64}\text{Mn}_2\text{O}_7$ with magnetic field. (a) and (b) are MFM images taken at the area shown in (c) at 78 K under different external fields: (a) 0 G and (b) 185 G. (c) is a topography with size $8.6 \times 8.6 \mu\text{m}^2$. (d) and (e) are MFM images taken at the area shown in (f) at 88 K under different external fields: (d) 0 G and (e) 240 G. (f) is a topography with size $7.3 \times 6.9 \mu\text{m}^2$. See text for details.

and 4(b), as can be seen by comparing the scale bars related to the MFM images. Upon applying a 240 G field, the in-plane domains do not change much, as seen in Fig. 4(e). The increase in contrast and brightness of the MFM images is mainly due to the increase in the magnetic moment of the MFM tip under the external field. The stripes marked by “T” in Fig. 4(e) represent tail-to-tail in-plane domains, which become clearer under a 240 G field. Possible closure domains are identified at the position marked by “C” in Fig. 4(e). These closure domains do not show any apparent change in response to the external field. Since the crystal $\text{La}_{1.36}\text{Sr}_{1.64}\text{Mn}_2\text{O}_7$ is a moderately uniaxial anisotropic ferromagnet at low temperatures,¹² the in-plane domains are expected to form in the (001) surface of the crystal due to demagnetizing fields exceeding the anisotropy, which was indeed observed by Konoto *et al.* using spin-polarized scanning electron microscopy.²⁴ We did not clearly observe the in-plane domains in this sample below 88 K due to the strong stray field generated by the out-of-plane domains.

IV. CONCLUSIONS

We have studied the magnetic structure of the $x=0.32$ compound at various temperatures in the absence or presence of an external magnetic field by using low-temperature MFM. We found that in the FM state, the FM domains with out-of-plane magnetization form treelike patterns below 88 K. These magnetic patterns remain highly stable below 65 K and start to undergo a gradual change with temperature above 65 K. As the temperature goes higher, more pro-

nounced changes in the domain patterns occur. At 88 K, in-plane domains were observed on the surface in the form of domain stripes and closure domains. Above 88 K, the in-plane domains gradually disappear as T_C is approached. The evolution of the FM domains occurs where the resistivity changes below T_C . We observed the SRT occurring around 74–88 K in our sample. The SRT is associated with the thermal evolution of the anisotropy energy, which reflects the two-dimensional character of the system. The significant change in the anisotropy energy with temperature is mainly due to a competition between the lattice elastic energy and the exchange striction. With increasing temperature, an orbital occupancy transition from $d_{3z^2-r^2}$ to $d_{x^2-y^2}$ is indicated by a decrease in the c/a ratio;²² however, the orbital transition itself is not related to the change in anisotropy energy because the $d_{3z^2-r^2}$ and $d_{x^2-y^2}$ orbitals do not contribute to the spin-orbit coupling due to the quenching of their orbital angular moment. We also observed large nanoscale changes in the magnetic structure upon thermal cycling, which may indicate short-range, two-dimensional ferromagnetic fluctuations in the basal plane.

ACKNOWLEDGMENTS

This work is supported by the National Science Foundation (DMR-0308575) and by the Welch Foundation (F-1533). Work carried out at Argonne National Laboratory was supported by the U.S. Department of Energy, Office of Science, under Contract No. DE-AC02-06CH11357.

*Present address: Beckman Institute, University of Illinois, Urbana, IL 61801.

†Present address: Physics Department, Cornell University, Ithaca, NY 14853.

‡Present address: Physics Department, Harvard University, Cambridge, MA 02138.

§Corresponding author; delozanne@physics.utexas.edu

¹A. Urushibara, Y. Moritomo, T. Arima, A. Asamitsu, G. Kido, and Y. Tokura, *Phys. Rev. B* **51**, 14103 (1995).

²P. Schiffer, A. P. Ramirez, W. Bao, and S.-W. Cheong, *Phys. Rev. Lett.* **75**, 3336 (1995).

³H. Y. Hwang, S.-W. Cheong, P. G. Radaelli, M. Marezio, and B. Batlogg, *Phys. Rev. Lett.* **75**, 914 (1995).

⁴John B. Goodenough and J.-S. Zhou, *Nature (London)* **386**, 229 (1997).

⁵J. M. De Teresa, M. R. Ibarra, P. A. Algarabel, C. Ritter, C. Marquina, J. Blasco, J. García, A. del Moral, and Z. Arnold, *Nature (London)* **386**, 256 (1997).

⁶M. Uehara, S. Mori, C. H. Chen, and S.-W. Cheong, *Nature (London)* **399**, 560 (1999).

⁷J. Mira, J. Rivas, F. Rivadulla, C. Vázquez-Vázquez, and M. A. López-Quintela, *Phys. Rev. B* **60**, 2998 (1999).

⁸John B. Goodenough, *J. Appl. Phys.* **81**, 5330 (1997).

⁹Liuwan Zhang, Casey Israel, Amlan Biswas, R. L. Greene, and Alex de Lozanne, *Science* **298**, 805 (2002).

¹⁰T. Kimura and Y. Tokura, *Annu. Rev. Mater. Sci.* **30**, 451 (2000).

¹¹J.-S. Zhou, J. B. Goodenough, and J. F. Mitchell, *Phys. Rev. B* **61**, R9217 (2000).

¹²U. Welp, A. Berger, V. K. Vlasko-Vlasov, Q. A. Li, K. E. Gray, and J. F. Mitchell, *Phys. Rev. B* **62**, 8615 (2000).

¹³T. Asaka, T. Kimura, T. Nagai, X. Z. Yu, K. Kimoto, Y. Tokura, and Y. Matsui, *Phys. Rev. Lett.* **95**, 227204 (2005).

¹⁴Tien-Ming Chuang and Alex de Lozanne, *Rev. Sci. Instrum.* **78**, 053710 (2007).

¹⁵Casey Israel, Changbae Hyun, Alex de Lozanne, Soohyon Park, and Z. G. Kim, *Rev. Sci. Instrum.* **77**, 023704 (2006).

¹⁶H. J. Williams, F. G. Foster, and E. A. Wood, *Phys. Rev.* **82**, 119 (1951).

¹⁷J. Unguris, M. R. Scheinfein, R. J. Celotta, and D. T. Pierce, *Appl. Phys. Lett.* **55**, 2553 (1989).

¹⁸J. B. Goodenough, *Phys. Rev.* **102**, 356 (1956).

¹⁹B. D. Cullity, *Introduction to Magnetic Materials* (Addison-Wesley, Reading, MA, 1972).

²⁰Changbae Hyun, Alfred K. H. Lee, and Alex de Lozanne, *Nanotechnology* **17**, 921 (2006).

²¹Q. A. Li, K. E. Gray, J. F. Mitchell, A. Berger, and R. Osgood, *Phys. Rev. B* **61**, 9542 (2000).

²²M. Kubota *et al.*, *J. Phys. Soc. Jpn.* **69**, 1606 (2000).

²³J. F. Mitchell (private communication).

²⁴M. Konoto, T. Kohashi, K. Koike, T. Arima, Y. Kaneko, T. Kimura, and Y. Tokura, *Phys. Rev. B* **71**, 184441 (2005).